



Magnetocaloric performance and its linear relationship with magnetoresistance in Gd-Al-Cu metallic glass

Jingtao Zhu^a, Qiang Luo^{a,b,*}, Minjuan Cai^b, Bin Ji^a, Baolong Shen^{b,c,*}

^a MOE Key Laboratory of Advanced Micro-structured Materials, School of Physics Science and Engineering, Tongji University, Shanghai 200092, China

^b School of Materials Science and Engineering, Jiangsu Key Laboratory for Advanced Metallic Materials, Southeast University, Nanjing 211189, China

^c Institute of Massive Amorphous Metal Science, China University of Mining and Technology, Xuzhou 221116, China

ABSTRACT

The magnetocaloric property and magneto-resistance (MR) of Gd₈₃Cu₉Al₈ metallic glass (MG) showing a second order ferromagnetic-paramagnetic transition have been investigated. A large maximum magnetic entropy change of 9.7 J/kg.K under a field change of 5 T was obtained, indicative of its attractiveness as magnetic refrigerants. Importantly, a linear relationship was observed between magnetic entropy change, ΔS_m , and MR in both the ferromagnetic and paramagnetic states, which is different from that of the reported rare earth based MGs and intermetallics. The diversiform relationships of MR vs ΔS_m in MGs imply the complexity of their underlying mechanisms. The linear ΔS_m -MR relationship sheds new light on the magnetocaloric effect of MGs, and can guide the design of amorphous magnetic refrigerants.

Over the last two decades, magnetocaloric effect (MCE) of amorphous alloys has attracted increasing interest owing to the totally disordered structure and second order magnetic transition nature [1–5,9–13,14]. These characteristics endow amorphous alloys with several advantages over crystalline materials as magnetic refrigerant, such as tunable magnetic transition temperature, high electrical resistivity, enhanced refrigeration capacity and little magnetic hysteresis [1–10]. The investigation of magnetocaloric performance of amorphous alloys mainly focuses on the Fe-based and rare earth based systems, whose magnetic ordering temperature covers from several Kelvin (in the Er-, Tm-based metallic glasses) to hundreds of Kelvin (in the Fe-based metallic glasses) [9–21]. Many amorphous alloy systems in different shapes (like wires, ribbons, powders and bulk rods) have been explored on the effects of alloying, crystallization, anisotropy, irradiation, demagnetization field and hydrogenation to tune their magnetocaloric performance [12–21]. And table like magnetic entropy changes can easily be obtained by using amorphous/amorphous or nanocrystalline/amorphous composite materials [2,6,12,15]. Furthermore, the scaling law of magnetic entropy changes under different field changes has been found, which can be used to prescreen MCE materials and to eliminate the contribution of minor magnetic phases, etc. [22–23]. And some models have been proposed to understand the MCE performance of some special amorphous alloy systems [24–25]. Recently, the maximum magnetic entropy change ($-\Delta S_m$) of a Gd-based metallic glass (MG) was shown to exhibit a power-law relation with the magnetoresistance (MR) above its Curie temperature (T_c), and a linear relationship

below T_c [26]. However, a power law relationship was found in an Er-based MG below T_c [21]. Although significant progress has been made concerning the magnetocaloric performance of amorphous alloys, the structural complexity makes the nature of MCE in amorphous alloys poorly understood compared with that of crystalline magnets.

In this article, we investigated the magnetocaloric behaviors and MR in Gd₈₃Cu₉Al₈ MG, which contains one magnetic element and has negligible random magnetic anisotropy due to spin orbit coupling of Gd [12,18]. A large maximum $|\Delta S_m|$ of 9.7 Jkg⁻¹ K⁻¹ was obtained under a field change of 5 T. Significantly, a linear relationship between MCE and MR is found in a wide temperature range but with different slopes in different temperature ranges above and below T_c . Furthermore, the external field effects the linear MCE-MR relationship differently above and below T_c . The linear relationship observed here is different from those reported in some Gd- and Er-based MGs [21,26].

The Gd₈₃Cu₉Al₈ (at. %) MG ribbon was first prepared by arc melting pure Gd, Al and Cu in an argon atmosphere. Then ribbons with a width of 3 mm and a thickness of 33 μ m were produced by melt spinning method at a speed of 35 m/s. The structure was investigated by x-ray diffraction (XRD) using Co-K α radiation. Thermal analysis was performed with a Perkin-Elmer (DSC) DSC-7 differential scanning calorimeter (heating rate of 20 K/min) under a continuous argon gas flow. The magnetic properties and resistivity under different external magnetic fields were tested in Physical Properties Measurement System, PPMS Model-9 of Quantum Design Company. For all the magnetic measurement, the magnetic field was applied parallel to the surface of

* Corresponding authors at: School of Materials Science and Engineering, Jiangsu Key Laboratory for Advanced Metallic Materials, Southeast University, Nanjing 211189, China.

E-mail addresses: q.luo@seu.edu.cn (Q. Luo), blshen@seu.edu.cn (B. Shen).

<https://doi.org/10.1016/j.jmmm.2020.166828>

Received 12 November 2019; Received in revised form 21 February 2020; Accepted 26 March 2020

Available online 27 March 2020

0304-8853/ © 2020 Published by Elsevier B.V.

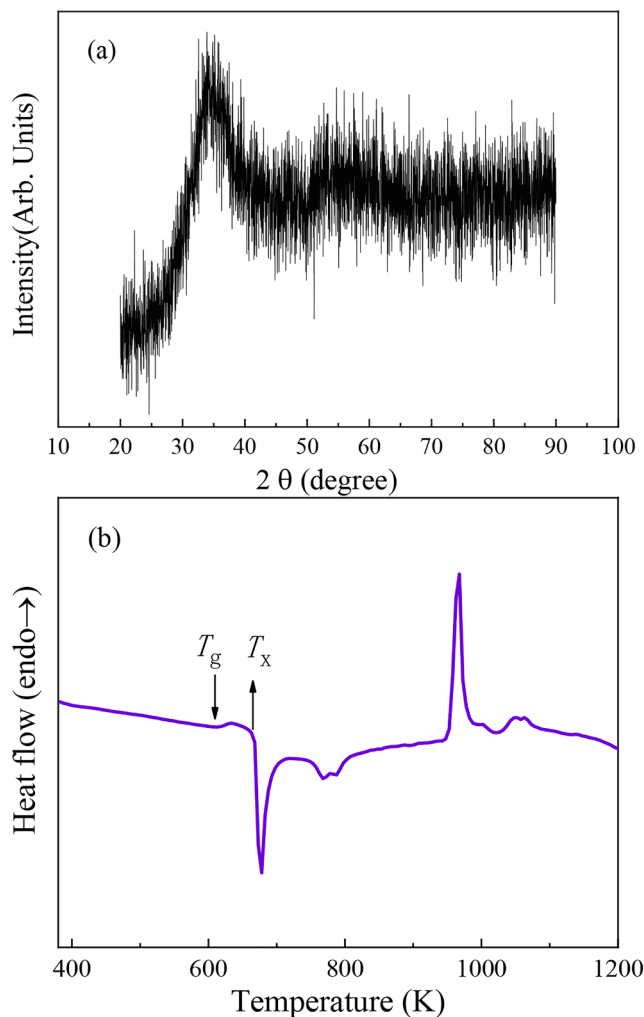


Fig. 1. (a) XRD pattern of the as-spun ribbon, (b) the DSC curve determined using a heating rate of 20 K/min.

amorphous ribbon, therefore demagnetization factor can be negligible.

Fig. 1(a) presents the XRD pattern of the $\text{Gd}_{83}\text{Cu}_9\text{Al}_8$ MG (as-spun state) with only very broad humps, indicating the fully amorphous structure of the alloy within the sensitivity limitation of XRD. It is worthy pointing out that this alloy system does not have as good glass forming ability as the Gd-Al-Co series [12,27], since when the spinning speed was 25 m/s, the ribbon was found to be partially crystallized. The distinct feature of the DSC curve in **Fig. 1(b)** includes an endothermic event owing to glass transition, two exothermic events arising from crystallization and a large endothermic peak due to melting. The onset temperatures of the glass transition and the first crystallization event of $\text{Gd}_{83}\text{Cu}_9\text{Al}_8$ were determined to be 615.8 K and 667.5 K, respectively, which resulted in a large supercooled liquid region of 52.0 K indicating its high thermal stability. **Fig. 2** presents the zero field cooled (measured on heating after cooling from 350 to 20 K in zero field) and field cooled magnetization curves (measured after cooling in 500 Oe) under a field change of 500 Oe, revealing little difference of both curves. This

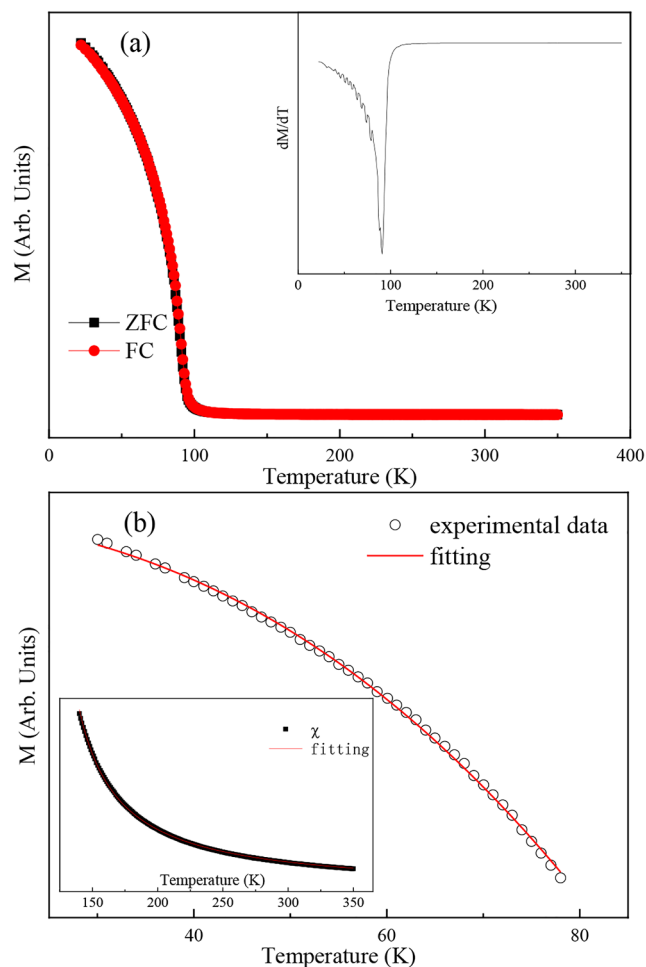


Fig. 2. (a) Zero field cooled and field cooled magnetization curves under 500 Oe, the inset shows the temperature dependence of dM/dT . (b) MT data and the fitting curve below T_c , the inset show the magnetic susceptibility above T_c and fitting data according to the Curie's law.

indicates that there exists only a simple paramagnetic-ferromagnetic transition without any spin glass like freezing process or any other magnetic transition. The Curie temperature T_c determined by the method shown in the inset of **Fig. 2** is found to be 91.0 K, which is close to those of many other Gd-based bulk MGs with lower Gd content [12,27]. In addition, it is found that in the low temperature ferromagnetic state the magnetization of present alloy follows very well the Bloch's relation [26]: $M(T) = M(0)(1 - B^*T^{3/2} - C^*T^{5/2})$, further indicating its ferromagnetic nature and existence of spin wave excitation in the magnetic state. And at higher temperature above T_c , the MT curve can be well fitted to the Curie's law, and then the effective paramagnetic moment and the paramagnetic Curie temperature to be $7.8 \mu_B$ and 111.7 K, respectively.

To obtain ΔS_m , a set of isothermal magnetization curves were measured from 0 to 50 kOe between 40 and 150 K and shown in **Fig. 3**. Well below T_c , the magnetization increases rapidly in a very narrow field range but approaches saturation very slowly with further increasing magnetic field, which shows obvious ferromagnetic character like other

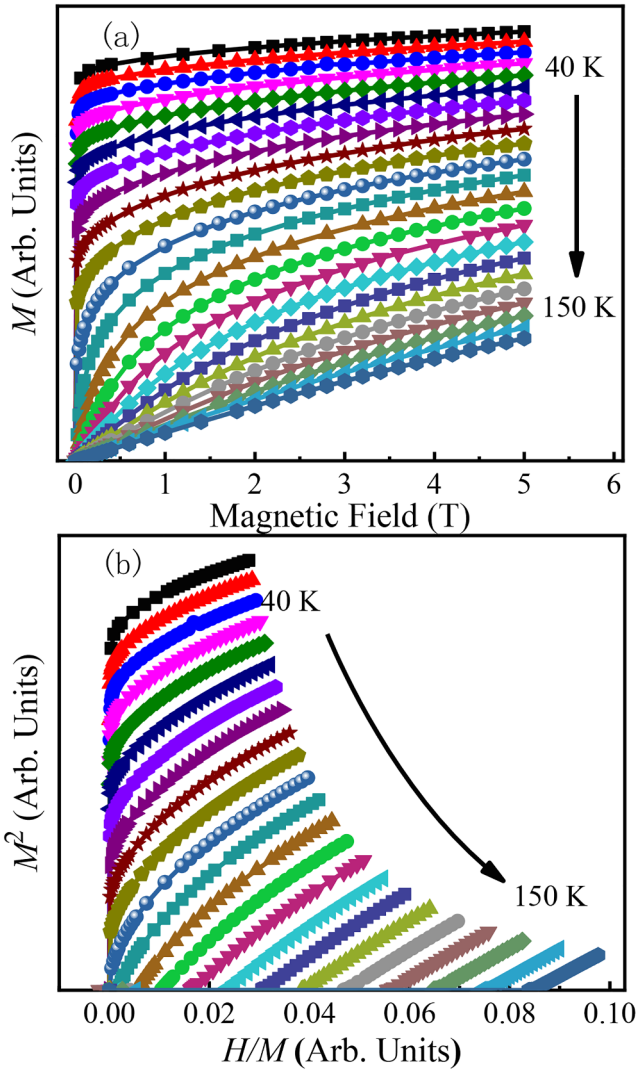


Fig. 3. (a) Typical isothermal magnetization curves between 40 and 160 K, and temperature step of 5 K is used. (b) The Arrott plot.

Gd-based amorphous alloys [12]. Fig. 3 (b) shows that the slopes of the Arrott plot are positive and there exists no inflection point, indicating the second-order magnetic transition nature. This feature is similar to other Gd-based MGs with ferromagnetic transition, but different with a Ho-based MG showing spin glass like freezing process [3,28]. Then $-\Delta S_m$ of the sample can be evaluated by using the thermodynamic Maxwell relation. As presented in Fig. 4 (a), the $-\Delta S_m$ increases with increasing the external field change, but remaining the shape and peak position almost unchanged, which is a typical feature for a material with second order ferromagnetic transition. The maximum $-\Delta S_m$ under 5 T is around 9.7 J/kgK at 95 K, which is comparable with those of other Gd-based MGs and much larger than those of Fe-based MGs [9,22,29]. It is also

noted that the maximum of $|\Delta S_m|$ is much larger than that of another Gd-Al-Cu MG [30], which is related to higher Gd content and larger exchange interaction strength in present MG [12].

For a magnetic solid with a second order magnetic transition, a power-law relationship between the field and the peak $-\Delta S_m$ was suggested in the framework of mean field theory [1,15]: $|\Delta S_M^{pk}| \propto H^n$, where $|\Delta S_M^{pk}|$ is the maximum magnetic entropy change. This relationship was observed experimentally in many Fe- and rare earth-based amorphous alloys but with larger n values than the predicted value (2/3) [1,12,15,21]. The present Gd-Al-Cu system also obeys such a relationship with $n = 0.74$. The n value is comparable to that of many Fe-,Gd-based MG ribbons and smaller than those of many rare earth based bulk MG having larger degree of medium range order [1,12,15,21]. In addition, the relative cooling power, another key parameter frequently used to estimate the MCE, was simply estimated to be 814.8 J kg^{-1} from:

$$\text{RCP} = |\Delta S_M^{pk}| \times \delta T_{\text{FWHM}} \quad (1)$$

where δT_{FWHM} is the full width at half $|\Delta S_M^{pk}|$, showing the good refrigerant capacity of present alloy. Furthermore, we tried to construct a universal curve for the magnetic entropy changes under different fields by normalizing the $-\Delta S_m$ curves with respect to the $|\Delta S_M^{pk}|$ and using a normalized temperature θ defined as [22,23]:

$$\theta = \begin{cases} -(T - T_c)/(T_{r1} - T_c), & T \leq T_c \\ (T - T_c)/(T_{r2} - T_c), & T > T_c \end{cases} \quad (2)$$

T_{r1} and T_{r2} correspond to the temperatures of $0.6 \times |\Delta S_M^{pk}|$ (which has been widely used). As seen in Fig. 4 (c), a master curve is observed for present sample, which further evidences the second order magnetic transition nature and very small demagnetizing field effect (this is reasonable since ribbon sample was used and the measuring field is applied along the sample surface) [22,23]. We also tried to use one reference temperature, from which one can also get a similar master curve.

Recently a power-law relation between MR and $-\Delta S_m$ was found around and below T_f in an Er-based amorphous alloy with spin glass like freezing process [21]. In contrast, in a Gd-Al-Co-B MG with paramagnetic-ferromagnetic transition, a power law (linear) relation was obtained above (below) T_c [26]. The different correlation of ΔS_m vs MR between the Gd- and Er-based MGs suggests that magnetic configuration may have a strong impact on this kind of correlation. However, the mechanism of the MR-MCE relationship was still poorly understood in MGs. It is unclear whether the power-law/linear relation is universal for MGs showing a given kind of magnetic state. To throw some new light on this issue, the MR was measured for this MG and shown in Fig. 4 (d), which is positive and increases with increasing field. Interestingly, the temperature dependence of MR(=R(H)/R(0)-1) shows similarity with MCE in their shapes and peak positions. To obtain the relationship between MR and MCE quantitatively, the MR vs ΔS_M plot is presented in Fig. 5. It is found in a wide temperature range, the ΔS_M varies almost linearly with MR. But the relationship shows different variations with the field in different magnetic states. As seen in the Fig. 5 (a), below T_c , the ΔS_M vs MR curve at 5 T links up with that at 2 T, with a small difference between the two relationship curves. However, above the

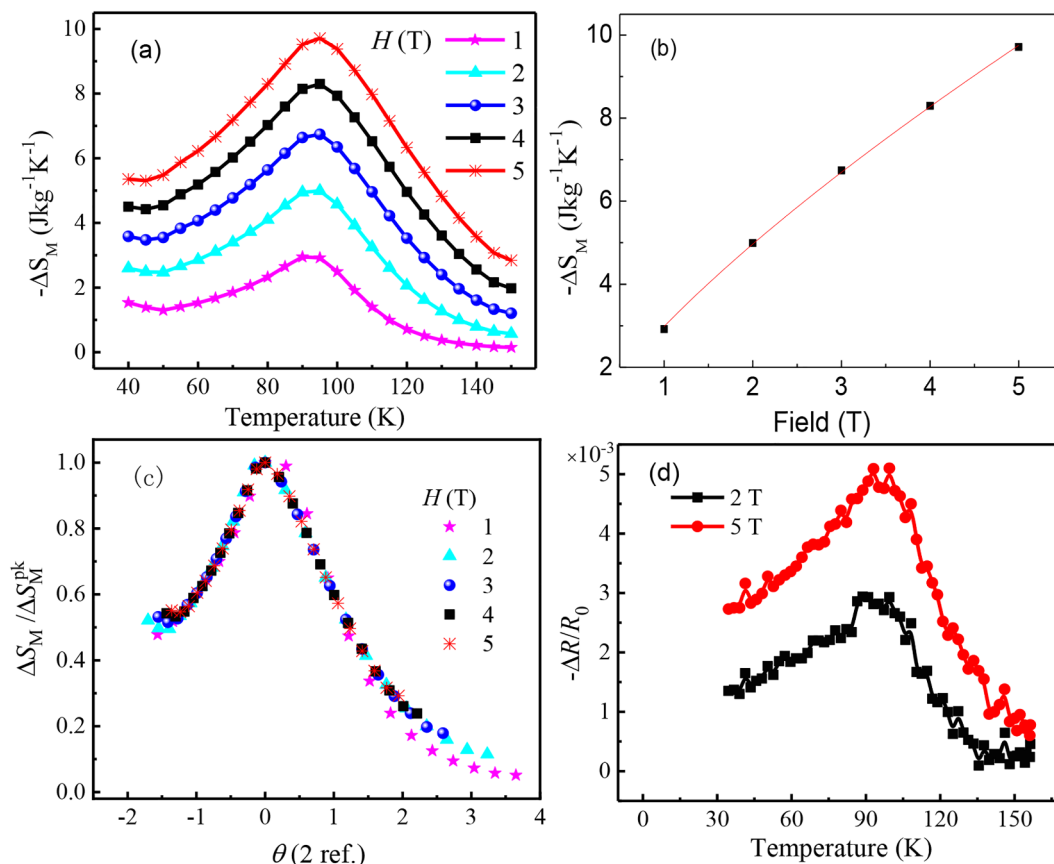


Fig. 4. (a) The magnetic entropy change under different field changes. (b) Field dependence of the peak magnetic entropy change. (c) Universal curves using two reference temperatures. (d) The temperature dependence of MR under fields of 2 T and 5 T.

Curie temperature, the ΔS_M vs MR curves obtained at 2 T and 5 T separates from each other obviously and have common ranges of $-\Delta S_M$ and MR. This can be ascribed to the different magnetic configurations in paramagnetic and ferromagnetic states. Thus, below T_c the present alloy shows different relationship with the Er-based MG, but similar to the Gd-Al-Co-B MG [21,26]. And above T_c , the linear relationship observed here is totally different from that of a previously reported Gd-based MG [26]. Note that the present MG also shows both similarity (above T_c) and difference (below T_c) with the $RA1_2$ (R:rare earth) compounds [31], where $MR \propto (T/T_c)^m |\Delta S_M|$ with $m = 1$ for $T < T_c$ and $m = 0$ for $T > T_c$. A model based on a Hamiltonian containing exchange, Zeeman and crystal field terms was used to make the calculations [31]. Interestingly, similar linear relationship was observed in $La_{0.6}Sr_{0.4}CoO_3$, $SrRuO_3$, and $CoPt_3$ above, at, and just below T_c , although they have different origins of ferromagnetism. And it was argued that the common origin of MR due to suppression of spin disorder was crucial for such a linear relationship [32]. These results of present

MG along with other MGs indicate that there does not exist a universal relationship of MGs even with the same type of magnetic ordering. In addition to the magnetic configuration, the short and medium range ordered atomic structures should play a significant role, which may explicate the differences of various MGs. Up to now, theoretical investigation of the correlations in MGs is still lacking, and the Handrich-Kobe model could be used to understand the mechanism in the future [33,34].

In conclusion, we investigated the MCE and MR of a Gd-Cu-Al MG with simple paramagnetic-ferromagnetic transition at ~ 91.0 K. A maximum $-\Delta S_m$ of $9.7 \text{ Jkg}^{-1} \text{ K}^{-1}$ and a maximum MR of 0.5% under 5 T were obtained around T_c . Significantly, it is found that ΔS_M is well scaled by MR due to the suppression of spin-disorder scattering in the whole investigated temperature range. The observed novel linear correlation between ΔS_M and MR both in the paramagnetic and ferromagnetic states enriches our understanding of the MR and MCE performance of amorphous alloys, and could be used to screen suitable

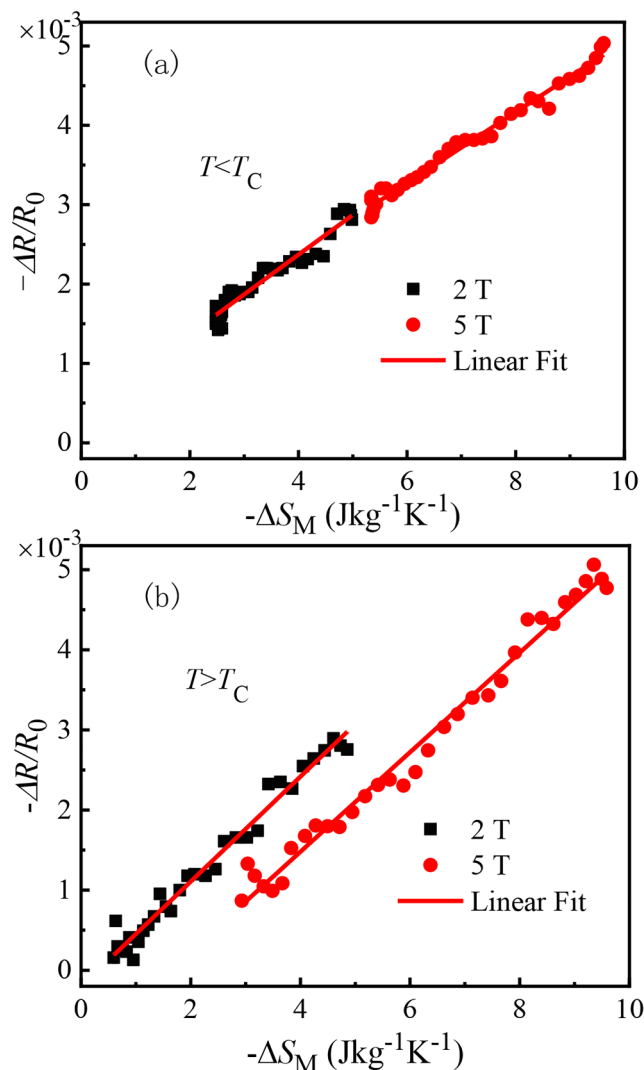


Fig. 5. (a) Relationship between MR and ΔS_M below the Curie temperature. (c) Relationship between MR and ΔS_m above T_C .

amorphous magnetocaloric materials.

Author statement

Jingtao Zhu and Qiang Luo designed experiments; Qiang Luo, Minjuan Cai and Bin Ji carried out experiments; Jingtao Zhu, Qiang Luo, Minjuan Cai, Baolong Shen analyzed experimental results. Qiang Luo, Jingtao Zhu and Baolong Shen wrote the manuscript with the

contributions from all other co-authors.

Acknowledgements

This work was supported by the National Natural Science Foundation of China (Grant Nos. 51971061, 11875204, 51631003 and 51371127), and the Fundamental Research Funds for the Central Universities (Grant Nos. 22120180070 and 2242019K40060).

References

- [1] V. Franco, J.S. Blázquez, J.J. Ipus, J.Y. Law, L.M. Moreno-Ramírez, A. Conde, *Prog. Mater. Sci.* 93 (2018) 112–232.
- [2] C.F. Sánchez-Valdés, et al., *Appl. Phys. Lett.* 104 (2014) 212401.
- [3] L. Xue, L.L. Shao, Q. Luo, B.L. Shen, *Intermetallics* 790 (2019) 633–639.
- [4] J. Li, L. Xue, W.M. Yang, C.C. Yuan, J.T. Huo, B.L. Shen, *Intermetallics* 96 (2018) 90–93.
- [5] B. Schwarz, B. Podmilsak, N. Mattern, J. Eckert, *J. Magn. Magn. Mater.* 322 (2010) 2298.
- [6] P. Álvarez, P. Gorria, J.L.S. Llamazares, J.A. Blanco, *J. Alloys Comp.* 568 (2013) 98–101.
- [7] K.A. Gschneider, V.K. Pecharsky, A.O. Tsokol, *Rep. Prog. Phys.* 68 (2005) 1479–1539.
- [8] F.X. Hu, B.G. Shen, J.R. Sun, Z.H. Cheng, G.H. Rao, X.X. Zhang, *Appl. Phys. Lett.* 78 (2001) 3675.
- [9] V. Franco, J.S. Blázquez, A. Conde, *Appl. Phys. Lett.* 88 (2006) 042505.
- [10] P. Álvarez, J.S. Marcos, P. Gorria, L.F. Barquín, J.A. Blanco, *J. Alloys Comp.* 504 (2010) s150–s154.
- [11] L. Xia, K.C. Chan, M.B. Tang, Y.D. Dong, *J. Appl. Phys.* 115 (2014) 223904.
- [12] Q. Luo, W.H. Wang, *J. Alloys Compd.* 495 (2010) 209.
- [13] H. Zhang, R. Li, L. Zhang, T. Zhang, *J. Appl. Phys.* 115 (2014) 133903.
- [14] H. Fu, M. Zou, Niraj K. Singh, *Appl. Phys. Lett.* 97 (2010) 262509.
- [15] Q. Luo, B. Schwarz, N. Mattern, J. Shen, J. Eckert, *AIP Adv.* 3 (2013) 032134.
- [16] H. Shen, H. Wang, J. Liu, E. Cao, F. Qin, D. Xing, D. Chen, Y. Liu, *J. Sun, J. Magn. Magn. Mater.* 372 (2014) 23.
- [17] F.X. Qin, N.S. Bingham, H. Wang, H.X. Peng, J.F. Sun, V. Franco, S.C. Yu, H. Srikanth, M.H. Phan, *Acta Mater.* 61 (2013) 1284–1293.
- [18] Q. Luo, B. Schwarz, N. Mattern, J. Eckert, *Phys. Rev. B* 82 (2010) 024204.
- [19] H.F. Belliveau, Y.Y. Yu, Y. Luo, F.X. Qin, H. Wang, H.X. Shen, J.F. Sun, S.C. Yu, H. Srikanth, M.H. Phan, *J. Alloys Compd.* 692 (2017) 658–664.
- [20] J.T. Huo, J.Q. Wang, W.H. Wang, *J. Alloys Compd.* 776 (2017) 202–206.
- [21] X.H. Kou, Q. Luo, J. Shen, *J. Alloys Compd.* 699 (2017) 591–595.
- [22] V. Franco, J.S. Blázquez, A. Conde, *Appl. Phys. Lett.* 89 (2006) 222512.
- [23] V. Franco, A. Conde, J.M. Romero-Enrique, J.S. Blázquez, *J. Phys. Condens. Matter* 20 (2008) 285207.
- [24] E.P. Nóbrega, et al., *J. Appl. Phys.* 113 (2013) 243903.
- [25] P.J. von Ranke, *J. Appl. Phys.* 116 (2014) 143903.
- [26] Q. Luo, J. Shen, *Intermetallics* 92 (2017) 79–83.
- [27] L. Xia, Q. Guan, D. Ding, M.B. Tang, Y.D. Dong, *Appl. Phys. Lett.* 105 (2014) 192402.
- [28] Q. Luo, B. Schwarz, N. Mattern, J. Eckert, *J. Appl. Phys.* 109 (2011) 113904–113908.
- [29] L.L. Shao, L. Xue, Q. Luo, Q.Q. Wang, B.L. Shen, *Materialia* 7 (2019) 100419.
- [30] Q.Y. Dong, B.G. Shen, J. Chen, J. Shen, J.R. Sun, *Solid State Commun.* 149 (2009) 417–420.
- [31] J.C.P. Campoy, E.J.R. Plaza, A.A. Coelho, S. Gama, *Phys. Rev. B* 74 (2006) 2952.
- [32] N. Sakamoto, T. Kyomen, S. Tsubouchi, M. Itoh, *Phys. Rev. B* 69 (2004) 092401.
- [33] K. Handrich, *Phys. Status Solidi* K55 (1969) 32.
- [34] J. Schreiber, S. Kobe, K. Handrich, J. Richter, *Phys. Status Solidi* 70 (1975) 673.